



HAL
open science

Highly stable and ultra-sensitive amperometric aptasensor based on pectin stabilized gold nanoparticles on graphene oxide modified GCE for the detection of aflatoxin M1

Amani Chrouda, Dhekra Ayed, Khaoula Zinoubi, Hatem Majdoub, Nicole Jaffrezic-Renault

► To cite this version:

Amani Chrouda, Dhekra Ayed, Khaoula Zinoubi, Hatem Majdoub, Nicole Jaffrezic-Renault. Highly stable and ultra-sensitive amperometric aptasensor based on pectin stabilized gold nanoparticles on graphene oxide modified GCE for the detection of aflatoxin M1. *Food Chemistry Advances*, 2022, 1, 10.1016/j.focha.2022.100068 . hal-03997226

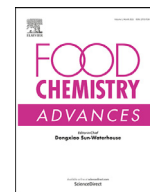
HAL Id: hal-03997226

<https://hal.science/hal-03997226>

Submitted on 20 Feb 2023

HAL is a multi-disciplinary open access archive for the deposit and dissemination of scientific research documents, whether they are published or not. The documents may come from teaching and research institutions in France or abroad, or from public or private research centers.

L'archive ouverte pluridisciplinaire **HAL**, est destinée au dépôt et à la diffusion de documents scientifiques de niveau recherche, publiés ou non, émanant des établissements d'enseignement et de recherche français ou étrangers, des laboratoires publics ou privés.



Highly stable and ultra-sensitive amperometric aptasensor based on pectin stabilized gold nanoparticles on graphene oxide modified GCE for the detection of aflatoxin M1



Amani Chrouda^a, Dhekra Ayed^b, Khaoula Zinoubi^b, Hatem Majdoub^b,
Nicole Jaffrezic-Renault^{c,*}

^a Department of Chemistry, College of Science at Zulfi, Majmaah University, Zulfi, 11952, Saudi Arabia

^b Laboratory of Interfaces and Advanced Materials, Faculty of Sciences, University of Monastir, Monastir, Tunisia

^c Institute of Analytical Sciences, UMR CNRS-UCBL 5280, 5 Rue la Doua, 69100, Villeurbanne Cedex, France

ARTICLE INFO

Keywords:

Aflatoxin M₁
Aptamer
Electrochemical sensor
Pectin
Differential pulse voltammetry

ABSTRACT

Herein, we have elaborated a new electrochemical aptasensor for the detection of ultra-trace amounts of aflatoxin M₁ (AFM₁) present in cow milk, with regulated low levels. To achieve detection of AFM₁, a simple strategy for the deposition of specific aptamers was elaborated, based on their grafting on pectin-reduced gold nanoparticles (AuNPs) electrogenerated on a graphene oxide sheet modified glassy carbon electrode. The elaboration of composite film was confirmed by cyclic voltammetry (CV), differential pulse voltammetry (DPV), electrochemical impedance spectroscopy (EIS), scanning electron microscopy (SEM), and UV-visible absorption measurements. The aptamer/pectin-AuNPs/GO/GCE exhibited significantly enhancement in the determination of AFM₁ in 20 min with a low detection limit 0.2 ng/L, a wide and useful linear range (10–1000 ng/L). An excellent stability, a high sensitivity, and a reproducibility as well as good recovery were obtained by the designed aptasensor. Moreover, the obtained results were tested in real samples. Thus, good electrochemical performance and simple preparation process of the aptamer/pectin-AuNPs/GO/GCE can provide promising potential for the detection of AFM₁ in milk samples in a daily use.

Introduction

Aflatoxins are produced by different fungi that widely exist in nature. The most toxic one is aflatoxin B₁ (AFB₁) which can be ingested by cows through contaminated feed (Min et al., 2021; Neal, Eaton, Judah & Verma, 1998). It is transformed into aflatoxin M₁ (AFM₁) through enzymatic hydroxylation of (AFB₁) at the 9a-position and has an approximate overall conversion rate estimated to 0.3 to 6.2% (Applebaum, Brackett, Wiseman & Marth, 1982; Cathey, Huang, Sarr, Clement & Phillips, 1994). AFM₁ is secreted in milk by the mammary gland of dairy cows, it is stable during the pasteurization, preparation and storage of various dairy products, and it is one of the most toxic contaminants in milk and milk derived products (Pandini et al., 2009). Therefore, AFM₁ contamination poses significant problems to human health, especially to children, who are the major consumers of milk, causing carcinogenicity which can provoke liver damage in humans as well as in animals (Bagchi, 2016; Galvano et al., 2001; Hampikyan, Bingol, Cetin & Colak, 2010). The legal regulations concerning AFM₁ concentrations in milk vary from country to country. The European Union allows a maximum level of AFM₁ 50ng/L in milk

(Roila et al., 2021). Regarding to AFM₁ human health contamination problems in worldwide, the development of simple, selective, sensitive and rapid tools for AFM₁ detection in real samples becomes an urgent request for the scientific community in the last decade.

Several methods have been established to overcome the problems of AFM₁ determination, such as high performance liquid chromatography (HPLC), enzyme linked immunoassay, liquid chromatography coupled with mass spectroscopy (LC-MS), and thin-layer chromatography (TLC) (Chavarría, Granados-Chinchilla, Alfaro-Cascante & Molina, 2015; Pei, Zhang, Eremin & Lee, 2009). However, most of these approaches have many limitations such as complicated pretreatment samples, time consuming analysis, expensive and cumbersome instruments and sensitivity or selectivity problems (Danesh et al., 2018; Nguyen, Flint & Palmer, 2019). To overcome these issues, various electrochemical approaches have been elaborated for AFM₁ detection.

The electrochemical biosensors are still considered the most widely reported, versatile, sensitive, and constitute an effective device for real time determination of AFM₁ level control (Nguyen et al., 2019). Classically, these tools involve the immobilization of specific antibodies, enzymes, or cells as a recognition element on the electrode sur-

* Corresponding author.

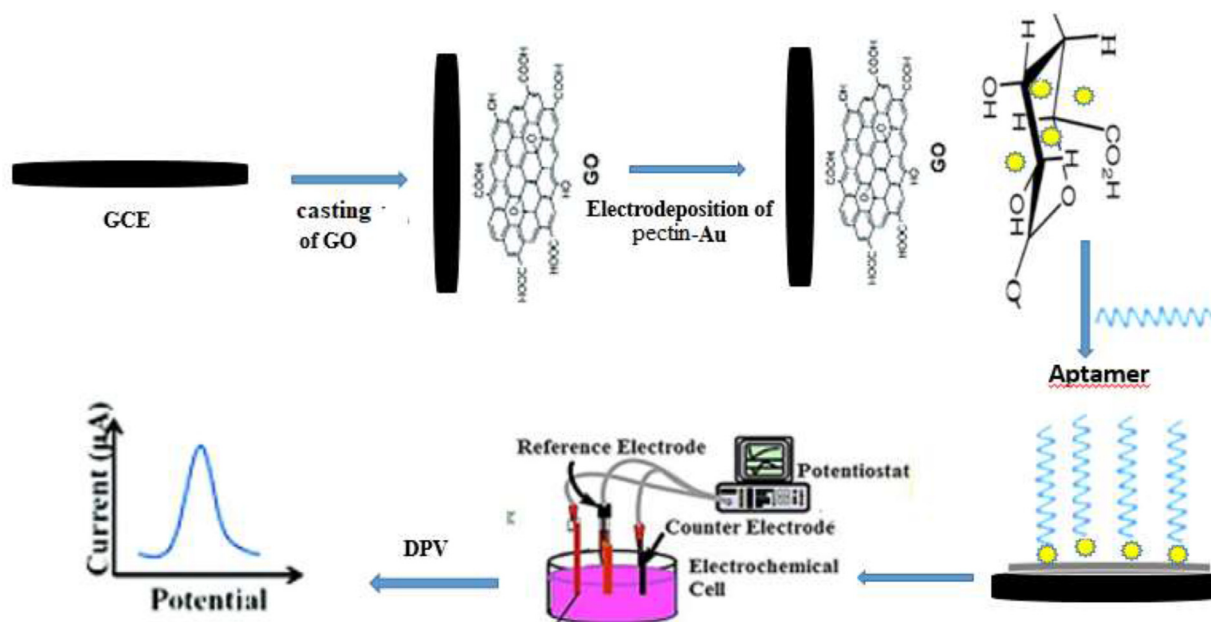


Fig. 1. Preparation of the aflatoxin M1 aptasensor.

face acting as a transducer. Nevertheless, due to the instability of these biological recognition pieces which consequently affects the biosensor performance, these devices are not applied as much as expected. Therefore the biological antibodies are often replaced by aptamers in various sensing platforms (Danesh et al., 2018; Istamboulié et al., 2016; Li et al., 2020; Song et al., 2020; Zhang et al., 2019). Aptamers are short synthetic nucleotide sequences, prepared by an in vitro process called SELEX (Cheng et al., 2020). They present a high affinity and specificity to a selected target, from small molecules to big proteins. Moreover, for the improvement of the sensitivity of aflatoxin detection, graphene sheets could be applied to provide extraordinary mechanical, thermal and electronic, properties (Muniandy et al., 2019). The application of nanoparticles is widely used for the construction of AFM₁ sensors, because of their extraordinary physico-chemical properties such as excellent electrocatalytic ability, large surface to volume ratio, and high conductivity (Hamami, Mars & Raouafi, 2021; Jalalian et al., 2018).

Nevertheless, still the disadvantage of nanoparticles agglomeration limits its application. To overcome these issues, biopolymers such as pectin have been used to inhibit aggregation, acting as a reducing agent and stabilizer (Al-Muhanna, Hileuskaya, Kulikouskaya, Kraskouski & Agabekov, 2015; Borker, Patole, Moghe & Pokharkar, 2017). In addition, pectin is a naturally polysaccharide, extracted from citrus peel, biodegradable, cheap, and non-toxic. Hydroxyl and carboxylic groups presented in pectin facilitate its interactions with nanoparticles and their reduction as well. Pectin has been used as a gelling agent, emulsifier, replacement of fats, stabilizer, thickening agent (Arora, Sood, Shah, Kotnala & Jain, 2016; Jauregui-Gomez et al., 2017; Kumari, JothiRajan & Mathavan, 2018).

Therefore, the conceptual idea of this study is to develop a new electrochemical sensor for an ultra-sensitive detection of AFM₁. The combination of graphene and pectin/nanoparticles with aptamers could present good electrocatalytic ability to the oxidation of AFM₁ and may display excellent sensor performance.

Experimental

Reagents

Aflatoxins are highly carcinogenic and must be handled with extreme care. Aflatoxin M1 contaminated labware should be decontaminated

with an aqueous solution of sodium hypochlorite (5%). Aflatoxins M₁ produced from *Petromyces albertensis*, graphite, pectin, gold (III) chloride trihydrate HAuCl₄·3H₂O (99.9%), and other chemicals were purchased from Sigma-Aldrich (Germany), and used without further purification. Aptamer (21-mer sequence 5'-NH₂-ACTGCTAGAGATTTCCACAT-3'), bearing a free amine at the 5' end was purchased from Biomers (Germany). All electrochemical experiments were performed in 5 mM phosphate buffer solutions (PBS, pH = 7.4) prepared with KH₂PO₄ and K₂HPO₄. All solutions were prepared with ultrapure water (resistivity >18 M.Ω.-cm) from a MilliQ purification system. Ethanol and acetone were purchased from Thermo Fisher.

Instrumentation

Cyclic voltammetry (CV) and electrochemical impedance spectroscopy (EIS) were carried out in electrochemical cell containing three electrodes connected to galvanostat/potentiostat system Autolab PG-STAT 302 N, controlled by Autolab software NOVA (v1.5) to design the data and experiments collection.

Scanning electron microscope images were performed by a field emission SEM (Merlin, Carl Zeiss). UV visible absorption measurements were carried out on a UnicoSpectro Quest 2800 spectrophotometer (Spain).

Electrochemical measurements

Glassy carbon electrodes were utilized as working electrode and it were polished using a 0.03 µm alumina slurry, and then washed with acetone, ethanol and water for 15 min. A platinum wire and an Ag/AgCl electrode were used as counter electrode and reference electrode respectively.

All electrochemical assays were performed in triplicate at room temperature. Cyclic voltammetry (CV) was carried out at scan rate equal to 25 mV/s, in the potential range (from -0.2 V to 0.6 V), in 0.1 M KNO₃ solution containing 5 mM of Fe(CN)₆^{3-/4-}, for each electrochemical characterization.

Aflatoxin M₁ aptasensor preparation

Graphite oxide layer which was prepared by Hummer's Method (Zaaba et al., 2017) then suspended in water. It was exfoliated to

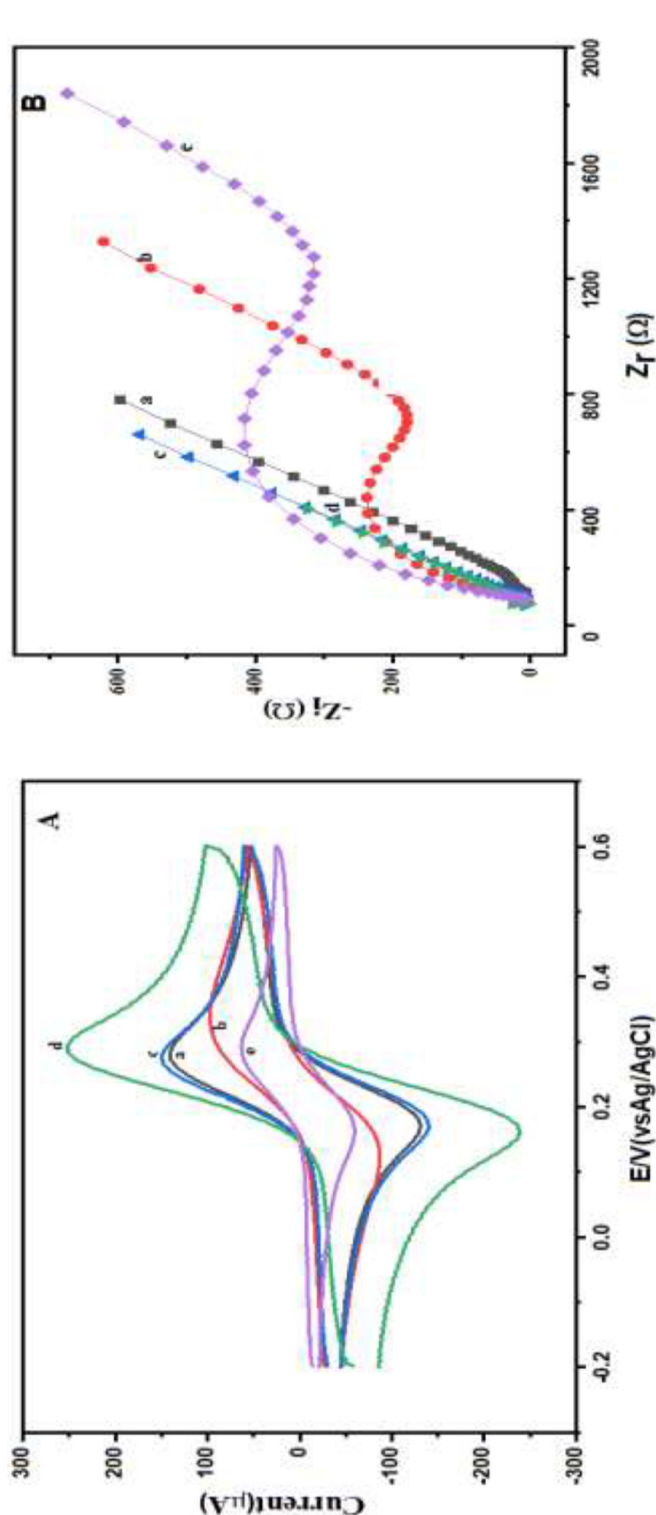


Fig. 2. (A). Cyclic voltammograms and (B) EIS of: bare GCE (a), GCE-pectin (b), GCE-pectin-AuNPs (c), and GCE-GO-pectin-AuNPs (d) in 5 mM $\text{Fe}(\text{CN})_6^{3-/4-}$.

1 mg/mL of graphene oxide (GO) film using ultrasonication (2 h). Then the GO was casted on the glassy carbon electrode surface.

Calcium chloride dehydrate and pectin (w/w: 1:2) were added to 5 ml of 0.1 M HCl solution, ultrasonicated for 15 min to get a uniform gel solution of pectin. Using cyclic voltammetry, electrodeposition of pectin at the glassy carbon electrode surface was carried out in the potential range of (0.0 V and -1.6 V). The prepared gel pectin (3 mg/mL) and HAuCl_4 (0.33 mg/mL) were mixed and ultrasonicated for 15 min. Moreover, the resultant (GO/GCE) surface was used for the electrodeposition of the pectin and AuNPs. Subsequently, the modified electrode was rinsed with ultrapure water. The anti-AFM₁ NH_2 -aptamer was grafted on the activated acid carboxylic groups on pectin via amide bond. For this, 5 μL of mixed NHS/EDC solution (10 mM) was dropped on the pectin functionalized working surface that was then dipped in 5 μL of 5 μM AFM₁ aptamer solution for 30 min. To remove the ungrafted aptamer and to passivate the surface, the developed aptasensor was immersed into 1% BSA solution and rinsed with ultrapure water (Fig. 1).

Results and discussion

Modification of the glassy carbon electrode (CGE)

Figure S1 exhibits the electrodeposition voltammograms of pectin film with and without the gold nanoparticles on the GO modified glassy carbon electrode. As visualized, in Fig. 2Aa successive decrease of the current density beyond potential of -0.5 V vs Ag/AgCl was observed, which could be explained by the reduction of protons at the glassy carbon electrode and thereby increase of pH at the electrode surface. At this range, the electrodeposition of pectin film has been taking place by the electrophoretic deposition. Furthermore, the pectin acid has apparent at pKa value 4.1. Above this pKa value, the surface charge of pectin decreases and pectin becomes insoluble due to strong interaction between the chains and is electrodeposited on the electrode surface.

On the other hand, figure S1B exhibits the voltammograms obtained by applying 10 cycles at scan rate of 25 mV/s in the presence of HAuCl_4 and in the potential range (-1.4 V, 1.4 V). During the forward scanning, Au^{3+} ions were reduced to gold nanoparticles, and anchored on the pectin film surface. The oxidation of gold nanoparticles appeared at potential 1.1 V and the reduction takes place at potential 0.5 V. The increase of peak currents density during the reduction and oxidation process confirmed the electrochemical deposition of gold nanoparticles on glassy carbon electrode (Al-Muhanna et al., 2015). The optimum amount of gold nanoparticles required has been obtained by tuning the number of electrodeposition cycles.

Electrochemical characterization of the GC surface modification

Electro catalytic activity at various modified electrode

Figure S2 displays the CVs of the electrode at bare GCE (a), GCE-pectin (b), GCE-pectin-AuNPs (c) and GCE-GO-pectin-AuNPs (d) films modified GCEs at the scan rate of 100 mV s^{-1} in 0.1 M KCl solution.

The voltammograms exhibited an oxidation peak at +1.20 V after the characterization of the GCE-pectin-Au this peak due to the gold nanoparticles presence. At the same potential, a current increasing after adding the graphene oxide to the modified surface was observe. Thus Go possess excellent conductance which improve the performance of the modified electrode.

Charge transfer properties

To control the surface modification, electrochemical impedance spectroscopy and cyclic voltammetry techniques were carried out in the presence of 5 mM $\text{Fe}(\text{CN})_6^{3-/4-}$ with 0.1 M of KCl, to characterize the charge transfer rate after each surface modification.

Fig. 2A exhibits a decrease of the oxidation peak current of the redox probe at (+0.32 V vs Ag/AgCl) after the pectin electrodeposition, which

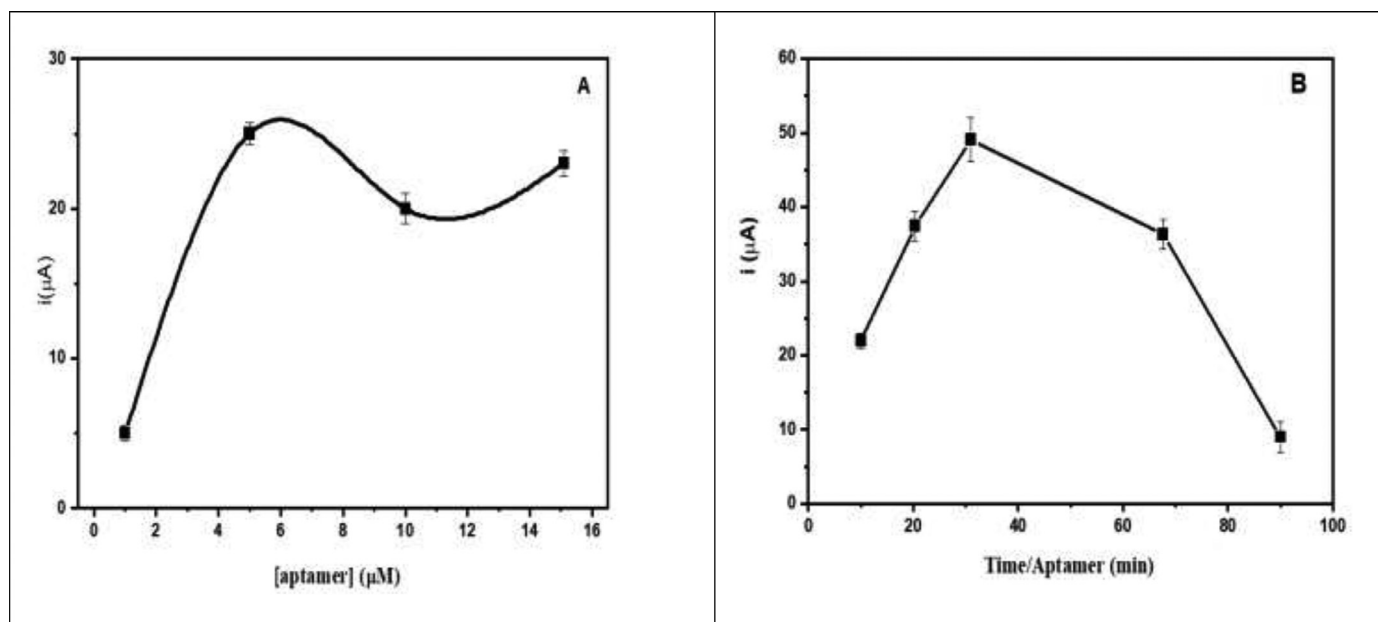


Fig. 3. Effect of (A) concentration of aptamer solution, (B) aptamer time, in 1.0 mM $\text{Fe}(\text{CN})_6^{4-/3-}$ with 0.1 M KCl solution. The error bars denote the standard deviation (SD) ($n = 3$).

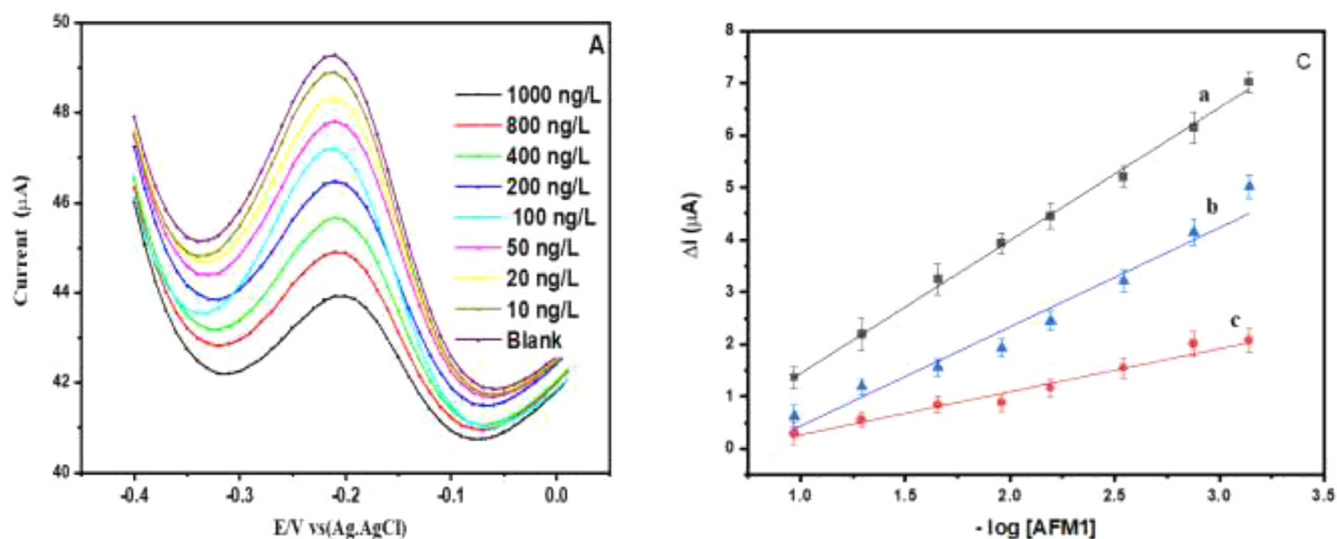


Fig. 4. A) differential pulse voltammogram (DPV) after adding different AFM₁ concentration ranging from 1000 pg/mL to 10 pg/mL. B) Effect of the pectin and AuNPs on the calibration plot of AFM₁ a) GCE-GO-AuNPs-pectin, b) GCE-GO-AuNPs, c) GCE-GO-pectin.

is attributed to the pectin poor conductivity; this modification was followed by a current increase due to the formation of gold nanoparticles. A massive increase of the peak current intensities is observed after adding the GO film to the surface, prior to pectin electrodeposition, due to the increase of electron transfer rate (Fig. 2A). The surface is ready for the aptamers immobilization. The anti-aflatoxin M₁ aptamer was covalently immobilized on the AuNPs/pectin/GO/CGE surface. These results were confirmed by the current intensity decrease after the aptamer incubation. To confirm these results, electrochemical impedance spectroscopy was also used for monitoring each surface modification.

For the electrochemical impedance spectroscopy (EIS) measurements (Fig. 2B), an alternative potential of low amplitude (5 mV) was used, in (10 mHz –100 kHz) frequency domain. The Nyquist plot data, indicates that the charge transfer resistance (R_{ct}) increases after pectin electrodeposition on the bare glassy carbon electrode (GCE) surface, confirming the results obtained by the cyclic voltammetry technique. Moreover, the gold nanoparticles incorporation leads to a decrease of

the R_{ct} value, due to the electrocatalytic properties of these nanoparticles. In agreement with the cyclic voltammetry results, a high electrical conductivity presented after adding the graphene oxide GO on the glassy carbon electrode, explained by small semicircle formed in the Nyquist plot with lower value of R_{ct} .

To present the appearing of gold nanoparticles (AuNPs), scanning electron microscope (SEM) images were carried out for the morphology characterization. Figure S3 presents the presence of agglomerated gold nanoparticles onto a glassy carbon electrode. While a typical rough electrode surface was obtained in the case of the bare glassy carbon, the AuNPs were well anchored and on the modified surface.

On the other hand, spectroscopic characterization was performed for pectin surface with and without gold nanoparticles to control its presence on the film surface. Figure S4 exhibited the UV-visible spectra of pectin film with and without gold nanoparticles. An intense peak appeared at 290 nm due to OH groups of pectin layer, this peak disappeared in the presence of gold nanoparticles because pectin carboxyl-

Table 1
Comparison of analytical performances of biosensors for AFM₁ detection.

Modified electrode	Linear range ng/L	LOD ng/L	AFM ₁ Incubation time (min)	Reference
FcTGL/AuNPs/SPCE nanoaptasensor	20–300	7.4	30	(Hamami et al., 2021)
DNA/Aptamer	20 to 200	5	30	(Stepanova et al., 2019)
CS-modified AuNPs/Aptamer	2 to 600	0.9	50	(S. H. Jalalian et al., 2018)
Biotinylated aptamers immobilized at neutravidin layer modified by ferrocene	15–120	8.47	60	(Karapetis, Nikolelis & Hianik, 2018)
Fe ₃ O ₄ /PANI/aptamer ss	6–60	1.98	–	(Nguyen et al., 2013)
HSDNA/AuNPs/ECNF	1–100	0.6	60	(Dinçkaya, Kınık, Altuğ & Akkoca, 2011)
AuNP/rGO/Aptamer	0.5–800	0.3	30	(Ahmadi, Hojatoleslami, Kiani & Molavi, 2022)
AuNPs/Zn/Ni-ZIF-8-800@graphene	180–1000	180	30	(Wang et al., 2022)
Aptamer/CCLP/GNPs/GO/GCE	10–1000	0.2	20	Our work

groups and other groups (-OH, =O) participate in the formation of zero-valence gold. The UV–Visible spectrum of pectin with AuNPs featured a typical absorption peak at 530 nm, attributed to the characteristic plasmon band of the AuNPs with a diameter of 23 nm.

Parameters optimization

To achieve the aptamer optimal concentration on the modified surface by GO/ AuNPs-pectin modified, the working electrode was coated with different aptamer concentrations (1, 5, 10 and 15 μ M) for an optimal time about 30 min, then DPV curve data was carried out in terms of aptamer concentration. As indicated in Fig. 3A, when increasing the aptamer concentration, the current value exhibited a decrease trend at concentrations higher than 5 μ M. After 5 μ M of aptamer, the electrode surface is well saturated with aptamer strands. Therefore, the concentration of 5 μ M was obtained as the optimal.

To select the optimal time of aptamer immobilization on the surface of the GO/pectin/AuNPs/GCE, the working electrode was modified with the aptamer solution after different time durations. As indicated in Fig. 3B, up to 30 min, all active sites on the electrode surface were saturated by the aptamer. Therefore, 30 min was selected as the optimal time to graft the aptamer on the modified working electrode surface.

Analytical performance of aflatoxin M₁ sensor

The response of the Aflatoxin M₁ based aptasensor was investigated by differential pulse voltammetry (DPV) in the potential range of -0.4 V to 0.0 V. Fig. 4A exhibits a decrease of intensity current peak of the Fe(CN)₆^{3-/4-} redox probe, according to an increase in aflatoxin M₁ concentrations from 10 ng/L to 1000 ng/L. This variation confirms the successful aptamer binding capacity towards target molecule with different concentrations.

In order to investigate the performance of the composite, the relative variation of the current peak intensities is proportional to -log [AFM₁]

concentrations in the dynamic range of 10 ng/L to 1000 ng/L. The sensitivity of the biosensor was determined in the presence and in the absence of pectin and/or gold nanoparticles to investigate the effect of each other on the sensor performance. The calibration curves (Fig. 4B) were plotted utilizing the difference in intensity data before and after AFM₁ addition, the sensitivity was estimated to be 1.86 μ A/pC for GCE-GO-pectin, 0.68 μ A/pC for GCE-GO-AuNPs, and 2.63 μ A/pC for GCE-GO-AuNPs-pectin. For GCE-GO-AuNPs-pectin, the limit of detection (LOD) is calculated to be 0.2 ng/L by $3\sigma/S$, where σ and S presented the standard deviation of the blank and the sensitivity, respectively.

Calibration curves presented in Fig. 4B show that the pectin layer plays a crucial role in ensuring the attachment of gold nanoparticles and reducing their size, which enhances the available surface area, the catalytic effect and the sensor performance.

To evaluate the designed AFM₁ sensor, the important analytical performance of the Aptamer/pectin-GNPs/GO/GCE, such as LOD, sensitivity and linear range towards aflatoxin M₁ detection are compared to those of other sensors based on aptamers published in the recent years (Table 1). The analytical performances of all the aptasensors are better than that of the immunosensors (Wang et al., 2022) in terms of detection limit.

According to the data presented in the Table 1, Ahmadi et al., elaborated an electrochemical AFM₁ aptasensor based on gold nanoparticles anchored on a graphene film. Their structure mentioned a detection limit 0.3 ng/L with a linear range of 0.5 ng/L to 800 ng/L but with incubation time 30 min and recovery percentage range about (90–108) and (91–111.5) [37]. In contrast, the same structure modified with pectin film (our work) exhibited a similar LOD (0.2 ng/L), but a wide linear range (10 ng/L-1000 ng/L), with less test time estimated to 15 min. This performance enhancement could be explained by the presence of pectin layer which play an important role to stabilize gold nanoparticles and rearrange their immobilization. Therefore, the proposed strategy is a promising approach to a direct AFM₁ sensor design aiming towards ultrasensitive detection of AFM₁ in real samples.

Table 2
Determination of AFM₁ in real milk samples using the fabricated aptasensor.

Sample	spiked (pg.mL ⁻¹)	Found ^a (pg.mL ⁻¹)	Recovery ^b (%)
Raw milk	20	23.1 ± 2.5	115
	200	198.000 ± 0.095	99
Pasteurized full fat milk	20	25 ± 1.5	125
	200	210 ± 0.85	110

^a Mean of three measurements ± SD.

^b Recovery (%) = $[100 - (C_{\text{spiked}} - C_{\text{found}})/C_{\text{spiked}}] * 100$.

Selectivity, stability, reproducibility and repeatability

Before the real-time testing and to further investigate the performance of aflatoxin aptasensor, a selectivity study was performed using different interfering molecules including Ochratoxin B (200 ng/mL), Aflatoxin M1 (200 ng/mL), Aflatoxin B1 (200 ng/mL), under the same conditions used for aflatoxin M₁ detection and using a freshly prepared substrate for each interference experiment.

According to figure S5, the responses of the aptasensor to other interfering molecules were negligible compared to AFM₁, while the response to AFM₁ was significant. The obtained result demonstrated that the selectivity of the aptasensor based on pectin, due to its high affinity towards AFM₁ molecules, is acceptable for the practical applications.

Long-time storage stability was also investigated. Five modified electrodes of each type were performed and their responses were determined at irregular intervals over 30 days. The electrodes were rinsed with pure water and stored at +4 °C in 20 mM phosphate buffer solution (pH 7).

Figure S6 exhibited that the aptasensor was stable over a long period. After 30 days, only 15% of the initial value was lost and 85% remained after 30 days. The slight decrease of the aptasensor response obtained after 30 days could be explained by the progressive decrease of aptamer activity. However, it can be concluded that pectin biopolymer has a protecting and stabilizing effects on aptamer activity. In contrast to other research work using the same strategy but in the absence of pectin layer, Ahmadi et al., elaborated an AFM₁-aptasensor based of graphene oxide and gold nanoparticles, the results mentioned that 91% was remained after only 14 days [37].

Five electrodes were fabricated independently under the same conditions to measure reproducibility. Then using DPV technique, the current data were recorded in the presence of 200 ng/mL of aflatoxin M1. Based on the results, the relative standard deviation (RSD) was 8.9%, indicating a suitable reproducibility of the proposed method of fabrication.

Milk samples analysis

The aptasensors ready for a real time test; it was used to measure AFM1 in two milk samples, including full fat pasteurized milk and raw cow milk. As shown in Table 2, after the milk samples were spiked with AFM1. The final concentrations in spiked samples were firstly controlled using HPLC/MS/MS. The aptasensor present an average recovery of 115%, and 125% with the RSD ranging from 2.5%, and 1.5% for raw and full fat pasteurized milk respectively, for a concentration of 20 ng/L, AFM1 indicating that the aptasensor is capable of accurately measuring AFM1 in real samples.

Conclusion

In the present study, the aptasensor has not been yet utilized as biorecognition based on pectin with gold nanoparticles for AFM₁ detection. The main idea of the present work is the use of pectin as nanoparticles stabilizer and enhance the performance of the modified surface. The glassy carbon electrode modified with graphene oxide, pectine and gold nanoparticles was developed to identify aflatoxinM1 in milk samples. The obtained results exhibited that the proposed aptasensor based

on pectin has a high capability for detecting AFM₁ in milk samples compared to other approaches. Under optimal conditions, a wide linear range 10 ng/L-1000 ng/L and low LOD 0.2 ng/L were obtained for measuring AFM₁ using DPV technique. Additionally, the proposed strategy exhibited the proper reproducibility and repeatability, high sensitivity, and acceptable specificity to aflatoxin M1, with an appropriate stability.

Declaration of Competing Interests

The authors declare that they have no known competing financial interests or personal relationships that could have appeared to influence the work reported in this paper.

Acknowledgments

Region Auvergne Rhone Alpes is acknowledged for the Pack Ambition International Project, EMBAI #246413. CNRS is acknowledged for the IRP NARES. Campus France is acknowledged for the financial support through PHC Maghreb EMBISALIM.

Supplementary materials

Supplementary material associated with this article can be found, in the online version, at doi:10.1016/j.focha.2022.100068.

References

- Ahmadi, S. F., Hojjatoleslami, M., Kiani, H., & Molavi, H. (2022). Monitoring of Aflatoxin M1 in milk using a novel electrochemical aptasensor based on reduced graphene oxide and gold nanoparticles. *Food Chemistry*, 373, Article 131321. doi:10.1016/j.foodchem.2021.131321.
- Al-Muhanna, M. K. A., Hileuskaya, K. S., Kulikouskaya, V. I., Kraskouski, A. N., & Agabekov, V. E. (2015). Preparation of stable sols of silver nanoparticles in aqueous pectin solutions and properties of the sols. *Colloid Journal*, 77(6), 677–684. doi:10.1134/s1061933x15060022.
- Applebaum, R. S., Brackett, R. E., Wiseman, D. W., & Marth, E. H. (1982). Aflatoxin: Toxicity to dairy cattle and occurrence in milk and milk products - a review. *Journal of Food Protection*, 45(8), 752–777. doi:10.4315/0362-028x-45.8.752.
- Arora, V., Sood, A., Shah, J., Kotnala, R. K., & Jain, T. K. (2016). Synthesis and characterization of thiolated pectin stabilized gold coated magnetic nanoparticles. *Materials Chemistry and Physics*, 173, 161–167. doi:10.1016/j.matchemphys.2016.01.019.
- Bagchi, D. (2016). *Swaroop and A. food toxicology*. CRC Pres.
- Borker, S., Patole, M., Moghe, A., & Pokharkar, V. (2017). Engineering of pectin-reduced gold nanoparticles for targeted delivery of an antiviral drug to macrophages: In vitro and in vivo assessment. *Gold Bulletin*, 50(3), 235–246. doi:10.1007/s13404-017-0213-0.
- Cathey, C. G., Huang, Z. G., Sarr, A. B., Clement, B. A., & Phillips, T. D. (1994). Development and evaluation of a minicolumn assay for the detection of Aflatoxin M1 in milk. *Journal of Dairy Science*, 77(5), 1223–1231. doi:10.3168/jds.S0022-0302(94)77061-2.
- Chavarría, G., Granados-Chinchilla, F., Alfaro-Cascante, M., & Molina, A. (2015). Detection of aflatoxin M1 in milk, cheese and sour cream samples from Costa Rica using enzyme-assisted extraction and HPLC. *Food Additives & Contaminants: Part B*, 8(2), 128–135. doi:10.1080/19393210.2015.1015176.
- Cheng, L., Xu, C., Cui, H., Liao, F., Hong, N., Ma, G., et al. (2020). A Sensitive Homogenous Aptasensor based on Tetraferrocene labeling for thrombin detection. *Analytica Chimica Acta*. doi:10.1016/j.aca.2020.03.017.
- Danesh, N. M., Bostan, H. B., Abnous, K., Ramezani, M., Youssefi, K., & Taghdisi, S. M. (2018). Ultrasensitive detection of aflatoxin B1 and its major metabolite aflatoxin M1 using aptasensors: A review. *TrAC Trends in Analytical Chemistry*, 99, 117–128. doi:10.1016/j.trac.2017.12.009.
- Dinçkaya, E., Kınık, Ö., Sezgintürk, M. K., Altuğ, Ç., & Akkoca, A. (2011). Development of an impedimetric aflatoxin M1 biosensor based on a DNA probe and gold nanoparticles. *Biosensors and Bioelectronics*, 26(9), 3806–3811. doi:10.1016/j.bios.2011.02.038.
- Galvano, F., Galofaro, V., Ritieni, A., Bognanno, M., De Angelis, A., & Galvano, G. (2001). Survey of the occurrence of aflatoxin M1 in dairy products marketed in Italy: Second year of observation. *Food Additives and Contaminants*, 18(7), 644–646. doi:10.1080/02652030118086.
- Hamami, M., Mars, A., & Raouafi, N. (2021). Biosensor based on antifouling PEG/Gold nanoparticles composite for sensitive detection of aflatoxin M1 in milk. *Microchemical Journal*, 165, Article 106102. doi:10.1016/j.microc.2021.106102.
- Hampikyan, H., Bingol, E. B., Cetin, O., & Colak, H. (2010). Determination of aflatoxin M1 levels in Turkish white, kashar and tulum cheeses. *J. Food, Agric. Environ*, 8(1), 13–15.
- Istamboulié, G., Paniel, N., Zara, L., Granados, L. R., Barthelmebs, L., & Nogueir, T. (2016). Development of an impedimetric aptasensor for the determination of aflatoxin M1 in milk. *Talanta*, 146, 464–469. doi:10.1016/j.talanta.2015.09.012.
- Jalalian, S. H., Ramezani, M., Danesh, N. M., Aliboland, M., Abnous, K., & Taghdisi, S. M. (2018a). A novel electrochemical aptasensor for detection of aflatoxin M1

- based on target-induced immobilization of gold nanoparticles on the surface of electrode. *Biosensors and Bioelectronics*, 117, 487–492. doi:10.1016/j.bios.2018.06.055.
- Jalalian, S. H., Ramezani, M., Danesh, N. M., Alibolandi, M., Abnous, K., & Taghdisi, S. M. (2018b). A novel electrochemical aptasensor for detection of aflatoxin M1 based on target-induced immobilization of gold nanoparticles on the surface of electrode. *Biosensors and Bioelectronics*, 117, 487–492. doi:10.1016/j.bios.2018.06.055.
- Jauregui-Gomez, D., Bermejo-Gallardo, O. M., Moreno-Medrano, E. D., Perez-Garcia, M. G., Ceja, I., Soto, V., et al., (2017). Freeze-drying storage method based on pectin for gold nanoparticles. *Nanomaterials and Nanotechnology*, 7, Article 184798041769732. doi:10.1177/1847980417697328.
- Karapetis, S., Nikolelis, D., & Hianik, T. (2018). Label-free and redox markers-based electrochemical aptasensors for aflatoxin M1 detection. *Sensors*, 18(12), 4218. doi:10.3390/s18124218.
- Kumari, G. V., JothiRajan, M. A., & Mathavan, T. (2018). Pectin functionalized gold nanoparticles towards singlet oxygen generation. *Materials Research Express*, 5(8), Article 085027. doi:10.1088/2053-1591/aab001.
- Li, Y., Liu, D., Zhu, C., Shen, X., Liu, Y., & You, T. (2020). Sensitivity programmable ratiometric electrochemical aptasensor based on signal engineering for the detection of aflatoxin B1 in peanut. *Journal of Hazardous Materials*, 387, Article 122001. doi:10.1016/j.jhazmat.2019.122001.
- Min, L., Fink-Gremmels, J., Li, D., Tong, X., Tang, J., Nan, X., et al., (2021). An overview of aflatoxin B1 biotransformation and aflatoxin M1 secretion in lactating dairy cows. *Animal Nutrition*, 7(1), 42–48. doi:10.1016/j.aninu.2020.11.002.
- Muniandy, S., Teh, S. J., Appaturi, J. N., Thong, K. L., Lai, C. W., Ibrahim, F., et al., (2019). A reduced graphene oxide-titanium dioxide nanocomposite based electrochemical aptasensor for rapid and sensitive detection of Salmonella enterica. *Bioelectrochemistry (Amsterdam, Netherlands)*. doi:10.1016/j.bioelechem.2019.02.
- Neal, G. E., Eaton, D. L., Judah, D. J., & Verma, A. (1998). Metabolism and toxicity of aflatoxins M1 and B1 in human-derived in vitro systems. *Toxicology and Applied Pharmacology*, 151(1), 152–158. doi:10.1006/taap.1998.8440.
- Nguyen, B. H., Tran, L. D., Do, Q. P., Nguyen, H. L., Tran, N. H., & Nguyen, P. X. (2013). Label-free detection of aflatoxin M1 with electrochemical Fe3O4/polyaniline-based aptasensor. *Materials Science and Engineering: C*, 33(4), 2229–2234. doi:10.1016/j.msec.2013.01.044.
- Nguyen, T., Flint, S., & Palmer, J. (2019). Control of aflatoxin M1 in milk by novel methods: A review. *Food Chemistry*, Article 125984. doi:10.1016/j.foodchem.2019.12598.
- Pandini, A., Tansini, G., Sigolo, S., Filippi, Laporta, L., Piva, M., & G (2009). On the occurrence of aflatoxin M1 in milk and dairy products. *Food and Chemical Toxicology: An International Journal Published for the British Industrial Biological Research Association*, 47(5), 984–991. doi:10.1016/j.fct.2007.10.005.
- Pei, S. C., Zhang, Y. Y., Eremin, S. A., & Lee, W. J. (2009). Detection of aflatoxin M1 in milk products from China by ELISA using monoclonal antibodies. *Food control*, 20(12), 1080–1085. doi:10.1016/j.foodcont.2009.02.00.
- Roila, R., Branciarri, R., Verdini, E., Ranucci, D., Valiani, A., Pelliccia, A., et al., (2021). A study of the occurrence of aflatoxin M1 in milk supply chain over a seven-year period (2014–2020): Human exposure assessment and risk characterization in the population of central Italy. *Foods (Basel, Switzerland)*, 10, 1529. doi:10.3390/foods10071529.
- Song, J., Huang, M., Jiang, N., Zheng, S., Mu, T., Meng, L., et al., (2020). Ultrasensitive detection of amoxicillin by TiO2-g-C3N4@AuNPs impedimetric aptasensor: Fabrication, optimization, and mechanism. *Journal of Hazardous Materials*, 391, Article 122024. doi:10.1016/j.jhazmat.2020.122024.
- Stepanova, V., Smolko, V., Gorbachuk, V., Stoikov, I., Evtugyn, G., & Hianik, T. (2019). DNA-poly lactide modified biosensor for electrochemical determination of the DNA-Drugs and aptamer-aflatoxin M1 interactions. *Sensors*, 19(22), 4962. doi:10.3390/s19224962.
- Wang, N., Liu, Q., Hu, X., Wang, F., Hu, M., Yu, Q., et al., (2022). Electrochemical immunosensor based on AuNPs/Zn/Ni-ZIF-8-800@graphene for rapid detection of aflatoxin B1 in peanut oil. *Analytical biochemistry*, 650, Article 114710. doi:10.1016/j.ab.2022.114710.
- Zaaba, N. I., Foo, K. L., Hashim, U., Tan, S. J., Liu, W.-. W., & Voon, C. H. (2017). Synthesis of graphene oxide using modified hummers method: Solvent influence. *Procedia Engineering*, 184, 469–477. doi:10.1016/j.proeng.2017.04.118.
- Zhang, J., Fang, X., Wu, J., Hu, Z., Jiang, Y., Qi, H., et al., (2019). A micro interdigitated electrode based aptasensor for real-time and ultratrace detection of four organophosphorus pesticides. *Biosensors and Bioelectronics*, Article 111879. doi:10.1016/j.bios.2019.111879.